The effect of pH on *Marinobacter hydrocarbonoclasticus* denitrification pathway and nitrous oxide reductase

Cíntia Carreira[1,2], Rute F. Nunes[1], Olga Mestre[1], Isabel Moura[2], Sofia R. Pauleta*[1]

[1] Microbial Stress Lab, UCIBIO, REQUIMTE, Departamento de Química, Faculdade de Ciências e Tecnologia, Universidade Nova de Lisboa, Campus da Caparica, 2829-516 Caparica, Portugal.

[2] Biological Chemistry Lab, LAQV, REQUIMTE, Departamento de Química, Faculdade de Ciências e Tecnologia, Universidade Nova de Lisboa, Campus da Caparica, 2829-516 Caparica, Portugal.

Corresponding Author

Sofia R. Pauleta

Microbial Stress Lab, UCIBIO, REQUIMTE, Departamento de Química, Faculdade de Ciências e Tecnologia, Universidade Nova de Lisboa, Campus da Caparica, 2829-516 Caparica, Portugal.

E-mail: srp@fct.unl.pt

Tel. +351212948385, ext 10967

Fax +351212948550

Abstract

Increasing atmospheric concentration of N_2O has been a concern, as it is a potent greenhouse gas and promotes ozone layer destruction. In the N-cycle, release of N_2O is boosted upon a drop of pH in the environment. Here, *Marinobacter hydrocarbonoclasticus* was grown in batch mode in the presence of nitrate, to study the effect of pH in the denitrification pathway by gene expression profiling, quantification of nitrate and nitrite, and evaluating the ability of whole cells to reduce NO and N_2O. At pH 6.5, accumulation of nitrite in the medium occurs and the cells were unable to reduce N_2O. In addition, the biochemical properties of N_2O reductase isolated from cells grown at pH 6.5, 7.5 and 8.5 were compared for the first time. The amount of this enzyme at acidic pH was lower than that at pH 7.5 and 8.5, pinpointing to a post-transcriptional regulation though pH did not affect gene expression of N_2O reductase accessory genes. N_2O reductase isolated from cells grown at pH 6.5 has its catalytic center mainly as CuZ(4Cu1S), while that from cells grown at pH 7.5 or 8.5 has it as CuZ(4Cu2S). This study evidences that an *in vivo* secondary level of regulation is required to maintain N_2O reductase in an active state.

Keywords: Denitrification; Nitrous oxide reductase; "CuZ" center; acidic pH; *Marinobacter hydrocarbonoclasticus*; marine bacteria

Introduction

Nitrous oxide (N_2O) has an estimated half-life of 120 years in the atmosphere, being one of the major contributors to the greenhouse effect [1, 2]. Global analysis of N_2O emissions highlights that there has been an enhancement of this gas in the atmosphere in the last century due to biomass burning, combustion of fossil fuel and in particular from agriculture through the use of synthetic nitrogenous fertilizers [3-5]. In fact, 60 % of N_2O emissions come from soils [5]. Nevertheless, a perturbation in nitrogen balance of marine systems has also been observed due to the increase presence of fertilizers in drainage waters and inorganic nitrogen leaching to coastal seawaters and oceans [2, 6].

An increase in nitrogen-based compounds together with low oxygen tensions in these environments induces anaerobic metabolic processes, such as denitrification and anammox (pathways of the nitrogen cycle). In fact, many bacteria can switch from respiring oxygen to respiring nitrate (NO_3^-) and using N_2O as terminal electron acceptor, by activating the denitrification pathway [7]. This pathway, when complete, is a four-step process, with each step being catalyzed by a different metalloenzyme, in which nitrate is reduced to the inert dinitrogen gas (N_2) via nitrite (NO_2^-), nitric oxide (NO) and N_2O [8]. The genes required for this pathway include those encoding the catalytic subunits of the reductases - nitrate reductase (*narG* or *napA*), nitrite reductase (*nirS* or *nirK*), nitric oxide reductase (*c-norB* or *q-norB*) and nitrous oxide reductase (*nosZ*), as well as genes encoding various accessory proteins necessary for the biosynthesis and cofactor assembly in those reductases [9].

The last step of the denitrification pathway is catalyzed by nitrous oxide reductase (N_2OR), in which N_2O is reduced to dinitrogen and water, in a reaction involving two electrons and two protons [10]. The analysis of the *nosZ* operon in several genomes let to the division of these enzymes in two clades, Clade I and Clade II [11]. Clade I N_2ORs were the first to be isolated, and they have been the focus of most of the spectroscopic, kinetic and structural studies

reported in the literature. Clade II N_2OR are not so well characterized and are present in Gram-positive bacteria and in canonical non-denitrifiers [12].

N_2OR is a homodimeric enzyme containing two multicopper centers - a binuclear copper center [13], CuA, which is the electron transferring center and whose properties are similar to CuA center found in cytochrome *c* oxidase; and a tetranuclear copper-sulfide cluster named "CuZ" center, which is the catalytic center [14]. The four coppers of the catalytic center adopt a tetrahedral arrangement and each of them is coordinated by two histidine residues, with exception of Cu_{IV}, which has only one histidine ligand. These characteristics are common to Clade I and Clade II N_2OR, but in Clade II N_2OR isolated from *Wolinella succinogenes* there is an additional C-terminal domain containing a *c*-type heme, which is a quite unique feature of this enzyme [15].

Attending to the fact that *Marinobacter hydrocarbonoclasticus* N_2OR, the focus of this work, belongs to Clade I N_2OR, the spectroscopic and redox properties of these enzymes will be described, and from now on they will be referred only as N_2OR for simplicity.

N_2OR has been isolated with "CuZ" center in two different forms CuZ(4Cu2S) and CuZ(4Cu1S). Several studies have shown that these two forms of "CuZ" center differ in their kinetic, spectroscopic and redox properties [16-19], and also in its structure, with CuZ(4Cu2S) presenting a second sulfur atom in between Cu_I and Cu_{IV} [20].

CuZ(4Cu1S) has only been isolated in the [$1Cu^{2+}$-$3Cu^{1+}$] oxidation state, which is kinetically inert and characterized by a maximum absorbance band at 640 nm [21]. This form of "CuZ" center can be reduced to the [$4Cu^{1+}$] oxidation state, after a prolonged incubation (between 3-5 h) with reduced viologens [22-24], becoming catalytically competent with a high turnover number (k_{cat} = 321 s^{-1}) [22].

CuZ(4Cu2S) can be isolated in two oxidation states, [$2Cu^{2+}$-$2Cu^{1+}$] or [$1Cu^{2+}$-$3Cu^{1+}$], with the reduction potential of this redox pair being + 60 mV, at pH 7.5 [18, 25], but cannot be

reduced to the [$4Cu^{1+}$] oxidation state [16, 25]. In its reduced state, CuZ(4Cu2S) can react with N_2O but has a very low turnover number (k_{cat} = 0.6 h^{-1}) [16]. Spectroscopically, it is characterized by a maximum absorption band at 550 nm with a shoulder at 635 nm in the oxidized state, and a broad absorption band with a maximum at 670 nm in the reduced state [17, 18].

There has been a debate as whether the active form of N_2OR *in vivo* is one with "CuZ" center as CuZ(4Cu2S) or as CuZ(4Cu1S). In fact, N_2OR with CuZ(4Cu2S) has been isolated mainly under anoxic conditions [18], while the enzyme with CuZ(4Cu1S) has been isolated under oxic conditions [18, 21]. However, N_2OR with CuZ(4Cu1S) was also isolated from a double mutant in *Paracoccus denitrificans nosXnirX* [26] or from *Pseudomonas stutzeri* mutants in the accessory gene *nosR* [27]. In fact, it has been proposed that NosR (maturated by NosX, or by the ApbE homologue protein [28]), could be responsible for maintaining N_2OR in an active state, or involved in electron transfer to N_2OR [26].

The rate of denitrification and amount of N_2O released to the atmosphere is affected by different environmental factors [29], such as copper availability [30], temperature [31, 32], oxygen concentration [33, 34], pH [35-38], sulfide concentration and carbon dioxide [39]. In some cases, it leads to its arrest at different points, resulting in an incomplete denitrifying pathway, but remaining an energy conservation process. Under such conditions NO and/or N_2O might be released to the atmosphere [40, 41]. The release of N_2O from cultures or soils kept at low pH values has been attributed to incorrect assembly of N_2OR [35, 36, 42], though the enzyme has never been isolated from cells grown under such conditions.

The effect of pH on the denitrification pathway of the marine bacterium *Marinobacter hydrocarbonoclasticus* 617 is reported. The influence of cultivating the cells at pH 6.5 or 8.5 on the denitrification pathway was investigated in a bioreactor operating in batch mode under microaerobic conditions. Nitrate and nitrite concentrations were monitored and the rates of

reduction of exogenous NO and N_2O gases by the whole cells were analyzed throughout the growth. The expression of genes encoding the catalytic subunits of the enzymes of the denitrification pathway, as well as some accessory proteins were analyzed, during the growth at the two pH values. In addition, N_2OR was isolated, spectroscopic and kinetically characterized from cells grown at three different pH values (6.5, 7.5 and 8.5) to identify differences that could explain at the molecular level the release of N_2O from acidic (soils or aquatic) environments.

Materials and Methods

Materials

All the reagents used in this work were of the highest purity grade available from either Sigma-Merck. In the assays with NO and N_2O, a NO- or N_2O-water-saturated solution was prepared at 95.5 µM and 25 mM, respectively. The N_2O solution was prepared by degassing 5 mL of Milli-Q water for 30 min with argon in a sealed serum flask (sealed with a rubber septum and aluminum cap) followed by vacuum cycles, and then flushed with N_2O (> 95 % N_2O, Air Liquid) for 1 h. For the preparation of the NO solution, a 10 % (per mass) KOH solution was placed between the NO bottle (5 % NO/95 % He, Air liquid) and the Milli-Q water argon-saturated solution, to remove other nitrogen oxides from the NO gas, and the solution was flushed during 1 h with NO.

Growth of M. hydrocarbonoclasticus in the bioreactor

M. hydrocarbonoclasticus 617 was grown in artificial seawater (ASW) liquid medium [43] at 30 ºC in an open system using a 2-L or 10-L bioreactor with 0.75 % (w/w) sodium lactate, as carbon source, and 10 mM sodium nitrate, as an electron acceptor. In short, microaerobic

conditions were achieved with an aeration rate of 0.2 vvm, maintained throughout the growth, and the culture was stirred at 150 rpm for 5 h, and afterwards at 50 rpm until the end of the growth (48 h). pH was continuously controlled and automatically adjusted to pH 6.5 or 8.5, with 1 M HCl or 1 M NaOH. The oxygen level was monitored using an oxygen electrode (Hamilton). The growth experiments were performed at least in triplicate. Samples of 4-mL were collected during the 2-L bioreactor growth and used to: i) measure the optical density at 600 nm (OD_{600nm}); and quantify ii) gene expression; iii) nitrate and nitrite; iv) nitric and nitrous oxide reduction rates by whole-cells (see below). 10-L bioreactor was used to obtain cell mass for protein purification. The growths performed in the 10-L bioreactor were monitored through nitrate and nitrite quantifications and by measuring the ability of whole-cells to reduce NO and N_2O.

At the end of each growth the cells were harvested by centrifugation (Beckman Avanti J-26 XPI) at 7930 *g* for 15 minutes, 6 ºC. The pellet was resuspended in 50 mM Tris-HCl pH 7.6 (in a proportion of 1 g cells per mL of buffer), containing protease inhibitors (EDTA-free cOmplete Protease Inhibitor, Roche) and DNase I (Roche), and then degassed by bubbling argon prior to its storage at - 80 °C.

Nucleic acid extraction and cDNA generation

Samples of 1-mL were taken at different time-points from the bioreactor (operating at pH 6.5 or 8.5) and immediately frozen in liquid nitrogen, until further use. Total RNA was extracted using the Isolate II RNA mini kit (Bioline), according to the manufacturer's instructions. Genomic DNA was digested with DNase I and its removal confirmed by PCR. RNA integrity was evaluated by agarose gel electrophoresis and estimated by determining the A_{260nm}/A_{280nm} and A_{260nm}/A_{230nm} ratios. Each RNA sample (500 ng) was reversely transcribed immediately after its extraction, to generate the respective cDNA using the SensiFAST cDNA Synthesis

Kit (Bioline) and the following thermal cycling settings: 10 min at 25 °C, 15 min at 42 °C and 5 min at 85 °C. cDNAs were 1:100 diluted and kept at -80 °C. DNA used in standard curves was extracted from a sample of the bioreactor culture taken during the exponential phase, using the Isolate II Genomic DNA Kit (Bioline), according to the manufacturer's instructions.

Quantitative Real-Time PCR

Effect of pH on the expression of *M. hydrocarbonoclasticus* genes involved in the denitrification pathway (*narG*, *nirS*, *c-norB, nosZ, nosR, nosD, nosL*) and accessory genes (*MARHY1479, MARHY1380*, *pCuC (MARHY1049)* and *senC (MARHY0057*)) were analyzed by quantitative real-time PCR (*q*PCR). Primers were designed using Primer3 software [44] (Table S1 in Supplementary Material). In each reaction, specific primers (250 nM) for the target gene were used to amplify the cDNA (3 µL) using the SensiFAST™ SYBR No-ROX Kit (Bioline). Reactions were performed on a Corbett Rotor-Gene 6000 instrument (Qiagen) using the following thermal cycling conditions: 95 °C for 5 min followed by 40 cycles of 95 °C for 15 s and 60 °C for 30 s. Analysis of melting curves generated by the stepwise increase of the temperature from 60 °C to 95 °C, were used to verify the specificity of the amplified products. Gene expression levels were determined using the relative standard curve method [45]. Standard curves were prepared with genomic DNA, and the amount of cDNA of each gene was determined by conversion of the mean threshold cycle (C_t) value of its respective DNA curve [45]. Relative normalized expression values were determined by dividing the quantity obtained for each gene by the one obtained for the control gene (*16S rRNA*), as its expression remained stable throughout the different growth phases. Reactions were run at least in duplicate and a "no template" and "no transcriptase" (a reverse transcription reaction containing all reagents except the reverse transcriptase enzyme) controls were also included in each *q*PCR assay. Similar expression profiles were obtained for three biological replicates

performed at each pH, but since samples were not collected at the same time-points, the data for one representative experiment is presented.

Nitrate and nitrite quantifications

Nitrate and nitrite concentrations were determined in triplicate in the samples collected from each growth, using the Nitrate/Nitrite Assay kit (Sigma). This method, involving two separated reactions, one to detect nitrite and another to detect both nitrate and nitrite, was performed in a 96-well microplate following the manufacturer's instructions. The absorbance was measured at 540 nm in a VersaMax ELISA Microplate Reader.

Nitric oxide and nitrous oxide reduction rates by whole-cells

The ability of whole-cells to reduce exogenous NO and N_2O in the presence of reduced methyl viologen was followed at 600 nm, using a fiber-optic diode-array spectrophotometer (TIDAS), inside a glove box (MBraun). Assays for nitric oxide reduction were performed with constant stirring, by adding 40 µL of *M. hydrocarbonoclasticus* cell suspension, collected from the bioreactor at each time-point, to a quartz cuvette already containing 120 µM methyl viologen and 60 µM sodium dithionite in 100 mM Tris-HCl pH 7.6 (in a final volume of 1 mL). The nitric oxide reduction assay was initiated with the addition of 100 µL NO-saturated water (to a final concentration of 9.6 µM). A similar procedure was followed for the nitrous oxide reduction assay, but with 100 µM methyl viologen and 50 µM sodium dithionite in 100 mM Tris-HCl pH 7.6 (in a final volume of 1 mL), with the reaction being initiated immediately (without further incubation) by addition of 50 µL N_2O-saturated water, to a final concentration of 1.25 mM. Reduction assays by whole-cells were performed within 1-3 h after collecting the cell suspension, with the samples being kept at 4 °C during that period. Reduction rates were determined by subtracting the slope of the residual oxidation in

the absence of substrate to the initial slope after NO or N_2O addition. The activity was calculated taking into consideration the number of electrons involved in each reaction and is reported as micromoles of NO or N_2O reduced per minute per optical density ($\mu mol_{NO \text{ or } N2O} \cdot min^{-1} \cdot OD^{-1}$).

Purification of nitrous oxide reductase

The cell suspension obtained from the growth experiments performed at different pH values (6.5, 7.5 and 8.5) was diluted 5 times with cold distilled water (dH_2O) and 0.5 mM EDTA, under continuous stirring, and incubated for 30 min at room temperature. The suspension was then centrifuged during 1 h, 6 ºC at 32816 *g* in a Beckman Coulter centrifuge (Avanti J-26 XPI), and the periplasmic extract was loaded onto an anion exchange DEAE Fast Flow chromatographic column (Ø 2.6 cm x 28 cm), previously equilibrated with 10 mM Tris-HCl pH 8.0. After washing out unbound proteins, a linear gradient, from 0 to 500 mM NaCl in 10 mM Tris-HCl pH 8.0, was applied during 250 min, at 3 mL min^{-1} to elute the bound proteins. The fractions containing N_2OR were diluted 10 times with distilled H_2O and applied onto a second anionic exchange Source15-Q chromatographic column (Ø 2.6 cm x 13 cm), previously equilibrated with 10 mM Tris-HCl pH 8.0. A step gradient, from 0 to 300 mM NaCl in 10 mM Tris-HCl pH 8.0, was applied during 200 min at 4 mL min^{-1}. The N_2OR-containing fractions were combined, concentrated using a Vivacell (Sartorius) apparatus over a YM30 membrane at 4 ºC, under argon atmosphere and stored as small spheres in liquid nitrogen. Fractions were monitored during the purification by visible spectroscopy and SDS-PAGE (12.5 % Tris-Tricine polyacrylamide) to evaluate N_2OR purity (see Figure S1 in Supplementary Material).

The whole procedure, starting from the periplasm preparation to protein purification, was performed under anoxic conditions inside a glove box, with an atmosphere of 2 % H_2 in

Argon (Coy Laboratories) at room temperature. This procedure is known to maintain "CuZ" center unaltered.

Biochemical and spectroscopic characterization of nitrous oxide reductase

Total protein concentration was determined by the Lowry modified method [46], using bovine serum albumin as the standard protein.

The visible spectra of the isolated samples of *M. hydrocarbonoclasticus* N_2OR were recorded on a UV-1800 spectrophotometer (Shimadzu). N_2OR samples were reduced with either sodium ascorbate or sodium dithionite and oxidized with a solution of potassium ferricyanide (dithionite and ferricyanide solutions were prepared in 100 mM Tris-HCl pH 7.6). Nitrous oxide reductase concentration was determined based on the extinction coefficient of the dithionite reduced form, 3.5 mM^{-1} cm^{-1} for CuZ(4Cu1S) at 640 nm [21] or 4.0 mM^{-1} cm^{-1} for CuZ(4Cu2S) at 670 nm (this work), for the monomer.

Total copper content was estimated using the 2,2'-biquinoline modified assay [47] and/or ICP (Inductively Coupled Plasma) analysis.

The electron paramagnetic resonance (EPR) spectra of each N_2OR purified sample (~200 µM per monomer, in 100 mM Tris-HCl pH7.6) were recorded on a X-band Bruker EMX spectrometer equipped with a rectangular cavity (model ER 4102T) and an Oxford Instruments continuous liquid helium flow cryostat, operating at 30 K. Spectra were acquired with the following instrument settings: microwave frequency, 9.65 GHz; microwave power, 2 mW; gain, 1 x 10^5. The EPR spectra of each N_2OR purified sample was acquired for the as-isolated, ferricyanide-oxidized, and ascorbate-, dithionite- and methyl viologen-reduced forms, prepared inside a glove box (Mbraun).

Enzymatic activity of the isolated N_2OR

All the procedures to prepare the fully reduced N_2OR and activity assays were performed inside a glove box (MBraun) at room temperature. Activity assays were performed by monitoring the oxidation of the redox mediator, using a TIDAS diode-array spectrophotometer. In short, 70 nM N_2OR was incubated under anaerobic conditions with 100 µM methyl viologen and 50 µM sodium dithionite in 100 mM Tris-HCl pH 7.6 during 180 min. After this period, the assay was initiated by adding N_2O-saturated water to a final concentration of 1.25 mM and the oxidation of reduced methyl viologen was followed at 600 nm [21, 48]. Specific activity was determined through linear regression fitting of the oxidation curve immediately after substrate addition. A similar assay was performed using a dithionite reduced N_2OR (prepared as describe below), but without further incubation with reductants in the activity assay.

The activity using reduced cytochrome c_{552} as electron donor was determined, as described in [22]. In the assay, 60 µM N_2OR were reduced with 100 equivalents of reduced methyl viologen or 5 mM sodium dithionite in 100 mM Tris-HCl pH 7.6 for 3 h followed by desalting using a NAP-5 column (GE Healthcare) equilibrated with the same buffer. The assays were initiated by the addition of dithionite- or fully reduced 70 nM N_2OR to a cuvette containing 7-10 µM reduced cytochrome c_{552} and 1.25 mM N_2O-saturated water, in 100 mM Tris-HCl pH 7.6. Specific activities, either using methyl viologen or cytochrome c_{552} as electron donor, are reported as $\mu mol_{N2O} \cdot min^{-1} \cdot mg_{N2OR}^{-1}$.

Results

M. hydrocarbonoclasticus cells grown under denitrifying conditions at different pH values

M. hydrocarbonoclasticus cells were grown in a 2-L bioreactor operated in batch mode in the presence of 10 mM sodium nitrate and at low aeration rate (to attain microaerobic conditions), maintaining the pH of the growth media constant at either pH 6.5 or 8.5 (see Figure S1 in Supplementary Material). The growth curve of *M. hydrocarbonoclasticus* at pH 8.5 had a diauxic behavior with a growth rate of 0.135 ± 0.006 h^{-1} for the first 7 h (see Figure S1A in Supplementary Material), during which the oxygen level decayed rapidly. After 2 h of incubation the oxygen level became negligible and remained as such for the entire duration of the growth period (see Figure S1B in Supplementary Material).

The growth curve of *M. hydrocarbonoclasticus* at pH 6.5, exhibited a shorter exponential phase (4 h) but with a higher growth rate, 0.164 ± 0.014 h^{-1}, followed by a stationary phase until the end of the growth period (see Figure S1A in Supplementary Material). The oxygen level became negligible in the beginning of the exponential phase, but increased after time-point 5 h, reaching around 90 % and remaining at that value until the end of the growth period (see Figure S1B in Supplementary Material). At this pH, the culture ceased growing leading to a lower final OD_{600nm} (0.82 *versus* 2.11, for the growth at pH 6.5 and pH 8.5, respectively) (see Figure S1A in Supplementary Material), which resulted in a lower wet cell mass (4 g L^{-1} media for pH 6.5 *versus* 8 g L^{-1} for pH 8.5).

Gene expression during M. hydrocarbonoclasticus growth under denitrifying conditions at different pH values

The expression of genes involved in the denitrification pathway of *M. hydrocarbonoclasticus* cells grown under denitrifying conditions at pH 6.5 (Figure 1A) and 8.5 (Figure 1B) was analyzed by *q*PCR. Expression profiles showed that genes encoding the catalytic subunits of

denitrifying enzymes (*narG*, *nirS*, *c-norB* and *nosZ*) are expressed simultaneously at each pH (Figure 1A and 1B). However, the timing of maximum transcription was affected by pH, as maximum transcription levels occurred at time-point between 1 and 3 h for pH 6.5 (Figure 1A) and at 7 h for pH 8.5 (Figure 1B), which corresponded to the end of the exponential phase (Figure 1A and 1B). A similar result was observed by Carreira and colleagues in *M. hydrocarbonoclasticus* cells grown at pH 7.5, in which the maximum of expression occurred after 5 h of growth [49].

In cells grown at pH 7.5 (published work by Carreira and colleagues in [49]) and at pH 8.5, the expression levels of *narG* were lower than the ones of the other denitrification genes (Figure 1B). In cells grown at pH 6.5, the gene with the lower expression level was *nirS* (Figure 1A). The maximum expression level of *nirS* in cells grown at pH 6.5 had a 6-fold decrease when compared with its maximum expression level at pH 8.5 (Figure 1).

- Insert Figure 1 here -

The expression profile of genes encoding the accessory proteins, proposed to be involved in the biosynthesis of N_2OR copper centers or in the maintenance of its active state [28, 50-52], were also analyzed by *q*PCR during growth experiments at pH 6.5, pH 7.5 and pH 8.5, but no significant changes were observed in their expression levels, with the exception of *senC* that had a lower expression at pH 6.5 (Figure S3 in Supplementary Material). Another difference was the expression profile of *MARHY1380* (*M. hydrocarbonoclasticus nosX* homologue, see Figure S2A in Supplementary Material), as its maximum expression occurred at the same time point as the one of genes encoding the catalytic subunits of denitrifying enzymes at pH 6.5 (Figure 1A). For the growth experiments at pH 7.5 and 8.5, *MARHY1380* was still highly expressed during the first 3 h (Figure S2B and S2C in Supplementary Material), but the

maximum gene expression of the genes encoding the catalytic subunits of denitrifying enzymes occurred at 5 h, for the growth experiment performed at pH 7.5 (published data in [49]) and 7 h, for the growth experiment performed at pH 8.5 (Figure 1B). This might evidence a different regulatory mechanism between *MARHY1380* and the denitrifying genes.

Nitrate and nitrite concentrations and activity of nitric oxide reductase and nitrous oxide reductase

Free nitrate and nitrite were quantified along the growth to detect whether nitrate reductase (NaR) and cytochrome cd_1 nitrite reductase (cd_1NiR) were active in the cells, as these enzymes catalyze the reduction of nitrate and nitrite, respectively. The presence of the other two enzymes of the denitrification pathway (nitric oxide reductase (NOR) and N_2OR) was evaluated by the ability of the cells to reduce exogenous NO and N_2O through the oxidation of reduced methyl viologen as an electron donor (Figure 2).

The analysis of these data showed that, nitrate consumption started at the same time point (2 h), and that after 7-8 h of inoculation it was completely consumed (Figure 2). This indicated that nitrate was transported to the cytoplasm, and it was consumed at a similar rate, independently of the pH at which the cells were grown and that NaR was active in these cells. The decrease in nitrate concentration was concomitant with formation of nitrite, which reached a maximum value close to the initial nitrate concentration. In the growth experiment performed at pH 8.5, nitrite was completely consumed after ~ 10 h (during the initial stages of the second diauxic growth phase) (Figure 2B), similar to what was previously observed by Carreira and colleagues in cells grown at optimum pH (pH 7.5) [49]. However, in cells grown at pH 6.5, only 27 % of the total nitrite produced was consumed and consequently high levels of nitrite (around 6.2 mM) remained in the medium until the end of the growth period (40 h) (Figure 2A).

In fact, it was observed a lower amount of cd_1NiR in the periplasm of cells grown at pH 6.5, when compared to the one of cells grown at pH 7.5 and pH 8.5 (see Figure S5 in Supplementary Material in which it is presented the heme-stained SDS-PAGE of the normalized periplasm).

Cells grown at pH 8.5 were able to reduce external NO and N_2O. In fact, their ability to reduce NO started before complete consumption of nitrite (5 h), coincident with the time-point at which *c-norB* had already started to be transcribed. Similarly, these cells were able to reduce N_2O after 7 h of incubation and maintained this ability until the end of the growth period (Figure 2B). Since reduction of N_2O by the whole cells was detected, it is plausible to argue that the four steps of the denitrification pathway are carried out by *Marinobacter hydrocarbonoclasticus* cells when grown at pH 8.5. Indeed, the profile of denitrification metabolites (NO_3^- and NO_2^-), as well as the profiles of the reduction rates of NO and N_2O by whole-cells grown at this pH were similar to the profiles reported previously in *M. hydrocarbonoclasticus* cells grown at optimum pH (pH 7.5) [49].

Cells grown at pH 6.5 were able to reduce externally provided NO after 6 h of incubation, ability that was maintained until the end of the growth period but were unable to reduce externally provided N_2O (Figure 2A). This suggested that NOR was produced in an active form in these cells, while N_2OR was either absent or not active.

- Insert Figure 2 here -

Biochemical and spectroscopic characterization of nitrous oxide reductase

The effect of the pH of the growth media on the mature N_2OR was analyzed through biochemical and spectroscopic characterization of the isolated enzyme. Little is known about the mechanism of N_2O reduction *in vivo*. However, it is now clear that a slight acidification

(pH 6.5) in the growth medium of *M. hydrocarbonoclastic*us was sufficient to affect N_2O reduction *in vivo*.

However, this acidification of the growth media had no significant effect in the expression level of *nosZ* or of any other genes encoding proteins considered to be important for the copper center assembly and/or activity of N_2OR. Thus, to seek for an explanation for such drastic effect, N_2OR was isolated from cells grown at different pH values (6.5, 7.5 and 8.5, named here as $N_2OR_{6.5}$, $N_2OR_{7.5}$ and $N_2OR_{8.5}$, respectively).

The yield of N_2OR isolated from the periplasmic extracts differed between preparations, being higher for $N_2OR_{7.5}$ (0.5 ± 0.2 $mg_{N2OR} \cdot g_{cell}^{-1}$), than for $N_2OR_{6.5}$ (0.16 ± 0.02 $mg_{N2OR} \cdot g_{cell}^{-1}$, a three-fold lower yield) (Table 1). The amount of copper determined per $N_2OR_{7.5}$ (monomer) was close to the expected value (6 copper atoms per monomer), while $N_2OR_{6.5}$ and $N_2OR_{8.5}$ had a lower copper/protein ratio than expected (Table 1), due to a lower purity index (presence of other proteins), which decreased this ratio (see Figure S6 in Supplementary Material). In fact, since the molar extinction coefficients (*vide infra*) were determined based on copper content and the values obtained were similar to the ones listed in the literature for N_2OR from other microorganisms [11], it means that these three N_2OR preparations had their copper centers fully loaded.

- Insert Table 1 here -

The visible spectra of $N_2OR_{6.5}$ differed from that of either $N_2OR_{7.5}$ or $N_2OR_{8.5}$ (Figure 3). The as-isolated $N_2OR_{6.5}$ exhibited a spectrum with a maximum absorption band at 640 nm, characteristic of CuZ(4Cu1S) in the [$1Cu^{2+}$-$3Cu^{1+}$] oxidation state, with CuA center being mainly in the [Cu^{1+}-Cu^{1+}] oxidation state (Figure 3A, spectrum II). The spectrum of $N_2OR_{6.5}$ reduced with sodium ascorbate (data not show) or sodium dithionite did not differ

significantly from the one of the as-isolated form, corroborating that the enzyme was isolated with CuA center in the reduced state. Upon oxidation of $N_2OR_{6.5}$ with potassium ferricyanide, absorption bands at 480 nm, 540 nm and 800 nm were observed, characteristic of the oxidized CuA center, while the absorption band with the maximum at 640 nm did not change (Figure 3A). These spectroscopic features are characteristic of N_2OR isolated with "CuZ" center mainly as CuZ(4Cu1S) [53].

The features of the as-isolated $N_2OR_{7.5}$ (and $N_2OR_{8.5}$) visible spectra evidenced that both CuA and "CuZ" centers were in the reduced state (Figure 3C and 3E, spectra II). Both centers were fully oxidized by addition of potassium ferricyanide, with the visible spectra presenting absorption bands with maxima at 480 nm, 540 nm and 800 nm, and a shoulder at 635 nm (Figure 3C and 3E, spectra I). Upon reduction of $N_2OR_{7.5}$ with sodium ascorbate, CuA center was reduced, not contributing to the spectra and the features of the "CuZ" center become defined, with a maximum absorption band at 550 nm and a shoulder at 635 nm (data not shown). The spectra of the dithionite reduced $N_2OR_{7.5}$ and $N_2OR_{8.5}$ exhibited a single absorption band with a maximum around 670 nm (Figure 3C and 3E, spectra III). The properties of the absorption spectra described for $N_2OR_{7.5}$ and $N_2OR_{8.5}$ are characteristic of N_2OR isolated with "CuZ" center mainly as CuZ(4Cu2S) [53].

The X-band EPR spectra of these different N_2OR preparations were also acquired at different oxidation states by complete oxidation with potassium ferricyanide, or selectively reducing the copper centers with sodium ascorbate (data not shown), sodium dithionite (data not shown) or methyl viologen (Figure 3B, 3D and 3F).

The EPR spectrum of oxidized $N_2OR_{6.5}$ showed an axial signal, with $g_{\parallel} = 2.17$ and $g_{\perp} = 2.04$, and showed a low resolved pattern of seven hyperfine lines in the $A_{\parallel}$ region ($A_{\parallel} = 3.9$ mT) (Figure 3B, spectrum I). This pattern is explained by a delocalized electron (S = 1/2) between two coupled copper nuclei ($I = 3/2$), assigned to the mixed-valence [$Cu^{1.5+}$-$Cu^{1.5+}$] oxidation

state of CuA center. The broadening of the spectra is attributed to a delocalized electron on the CuZ(4Cu1S), in the [1Cu^{2+}-3Cu^{1+}] oxidation state. This form of "CuZ" center cannot be further reduced by sodium dithionite, but its signal disappeared upon prolonged incubation with reduced methyl viologen (Figure 3B, spectrum IV). This is an evidence that "CuZ" center was completely reduced to the [4Cu^{1+}] oxidation state, which is diamagnetic. These spectral features are similar to the ones previously reported for *M. hydrocarbonoclasticus* N_2OR with "CuZ" center mainly as CuZ(4Cu1S) [54], strengthening the conclusion taken from the analysis of its visible spectra.

The EPR spectra of oxidized $N_2OR_{7.5}$ (and $N_2OR_{8.5}$) presented an axial signal with $g_{\parallel}$ = 2.18 and $g_{\perp}$ = 2.03, with a well-resolved 7-line hyperfine coupling ($A_{\parallel}$ = 3.9 mT), in an intensity ratio of 1:2:3:4:3:2:1 (Figure 3D and 3F, spectra I). These features arise from the presence of the mixed-valence CuA center in the [$Cu^{1.5+}$-$Cu^{1.5+}$] oxidation state, as explained before. The well-resolved 7-line pattern in N_2OR EPR spectrum is generally observed when the only contribution to this spectrum is CuA center, suggesting that the form of "CuZ" center present in such sample is diamagnetic and in the [2Cu^{2+}-2Cu^{1+}] oxidation state. The EPR spectra of $N_2OR_{7.5}$ and $N_2OR_{8.5}$ after prolonged incubation with reduced methyl viologen exhibited an axial signal, similar to the sodium dithionite reduced sample (data not shown) but with lower intensity (Figure 3D and 3F, spectra IV), suggesting that methyl viologen could not reduce this form of "CuZ" center to the [4Cu^{1+}] oxidation state, in agreement with the previous observations that in these samples "CuZ" center was mainly as CuZ(4Cu2S) [16].

- Insert Figure 2 here -

The specific activity of each N_2OR preparation was determined in the presence of its physiological electron donor, cytochrome c_{552}, or an artificial donor, methyl viologen [22] (Table 2).

Knowing that N_2OR with CuZ(4Cu1S) is only active in the fully reduced form [16], the three enzyme samples were incubated with methyl viologen during 3 h, prior to measuring its activity. The specific activity of $N_2OR_{6.5}$ determined using this procedure (192 ± 14 $\mu mol_{N2O} \cdot min^{-1} \cdot mg_{N2OR}^{-1}$) was higher than the one of $N_2OR_{7.5}$ (51 ± 18 $\mu mol_{N2O} \cdot min^{-1} \cdot mg_{N2OR}^{-1}$) and $N_2OR_{8.5}$ (55 ± 5 $\mu mol_{N2O} \cdot min^{-1} \cdot mg_{N2OR}^{-1}$) samples (Table 2). This was an indication that the percentage of CuZ(4Cu1S) was higher in the enzyme isolated from cells grown at pH 6.5. Moreover, considering that an enzyme sample with 100 % of CuZ(4Cu1S) has a specific activity of 200 $\mu mol_{N2O} \cdot min^{-1} \cdot mg_{N2OR}^{-1}$ [16, 53], the data showed that $N_2OR_{7.5}$ and $N_2OR_{8.5}$ were isolated with around 25 % of CuZ(4Cu1S), even if all the purification procedure was performed in the absence of oxygen.

The activity corresponding to CuZ(4Cu2S) was measured in assays with N_2OR reduced with sodium dithionite, as CuZ(4Cu2S) in the [$1Cu^{2+}$-$3Cu^{1+}$] oxidation state is able to reduce N_2O, while CuZ(4Cu1S) in the same oxidation state is not, as previously reported [16]. The specific activity of dithionite-reduced $N_2OR_{7.5}$ is 0.15 ± 0.03 $\mu mol_{N2O} \cdot min^{-1} \cdot mg_{N2OR}^{-1}$ (Table 2), and considering that this enzyme preparation had 75 % of CuZ(4Cu2S), then 0.2 $\mu mol_{N2O} \cdot min^{-1} \cdot mg_{N2OR}^{-1}$ is the estimated specific activity for a preparation with 100 % of CuZ(4Cu2S).

In addition, the catalytic activity of $N_2OR_{6.5}$ and $N_2OR_{7.5}$ was investigated in the presence of its putative physiological electron donor, cytochrome c_{552}. A specific activity of 1.25 ± 0.07 $\mu mol_{N2O} \cdot min^{-1} \cdot mg_{N2OR}^{-1}$, was determined for the fully reduced $N_2OR_{6.5}$, while $N_2OR_{7.5}$ reduced with sodium dithionite exhibited a much lower value, 0.004 ± 0.001 $\mu mol_{N2O} \cdot min^{-1} \cdot mg_{N2OR}^{-1}$ (Table 2).

- Insert Table 2 here –

Discussion

Effect of pH in M. hydrocarbonoclasticus denitrification pathway

The observation of a diauxic growth at pH 8.5 is due to a limitation in the electron acceptor, as initially both oxygen and nitrate are being used by the cells, while in the second part of the growth, only nitrite is used as terminal acceptor. A similar behavior was reported for *P. denitrificans* Pd1222 grown anaerobically in the presence of 60 mM nitrate at pH 7.2 [55]. At pH 6.5, the accumulation of toxic byproducts due to the low pH (see below) lead to an early growth arrest (Figure S1A in Supplementary Material).

The pH of the growth media does not affect the global nitrate consumption by the cells, though in cells grown at pH 6.5 its consumption is slower. On the contrary, nitrite consumption changes with pH, indicating that nitrite reductase is being affected at pH 6.5, while in cells grown at pH 8.5 there is a clear correlation between *nirS* expression and the concentration of nitrite in the medium (Figures 1 and 2). At pH 6.5 nitrite concentration remains high until the end of the growth period (Figure 2), which can be explained by the 6-fold lower *nirS* expression relative to cells grown at pH 8.5 (Figure 1) and by the lower production of cd_1NiR in the cells grown at pH 6.5. This was confirmed by electrophoretic studies of the periplasm of cells grown at different pH values (see Figure S5 in Supplementary Material). The effect of acidifying the growth media in the amount of mature cd_1NiR was also reported in *P. denitrificans* grown at suboptimal pH 6.8, but in this case no differences were observed in *nirS* expression (relative to pH 7.5) [56]. A decrease in *nirS* expression level was only reported for this organism, in a growth performed at pH 6.0 [42, 56]. However, in that case the authors also reported lower values of *norB*, *nosZ* and *nirS* transcripts (*narG* quantification was not reported) relative to the growth at pH 7.0, with *nosZ/nirS* and *nosZ/norB* ratios not being significantly affected [42]. In the present study, *c-norB* and *nosZ* genes relative expression were also affected by the pH of the growth media,

with a 2-fold lower expression in cells grown at pH 6.5 compared to the ones at pH 8.5, while for *nirS* there was a 6-fold decrease. Thus, *nosZ/nirS* ratio is significantly affected in cells grown at pH 6.5, whereas *nosZ/c-norB* ratio is not (see Figure S4 in Supplementary Material). The observed nitrite accumulation in *M. hydrocarbonoclasticus* grown at pH 6.5 led to the formation of 4.3 μM nitrous acid (HNO_2) in the medium. The accumulation of this acid was also reported in acidic cultures of *Pseudomonas fluorescens* and *P. denitrificans* upon nitrite accumulation [56-58], and explains the inactivation of cd_1NiR and also the growth arrest observed at acidic suboptimal pH values in the presence of nitrite. Moreover, HNO_2 dissociates into reactive species, such as nitric oxide and nitroxyl anion intermediates [59], explaining the NO accumulation in *P. denitrificans* cultures grown at acidic pH values [42]. Thus, although in *M. hydrocarbonoclasticus* grown at pH 6.5, *nirS* transcription stops after 10 h, and cd_1NiR is produced at lower levels, NO can be chemically formed. Under such conditions, NO-induced transcription of the denitrifying genes can occur through the DNR-type regulator [33, 34] (that in *M. hydrocarbonoclasticus* is encoded by *MARHY3023*).

Although cells grown at pH 6.5 and 8.5 have the ability to reduce added NO, indicating the presence of a functional NOR, major differences were observed in N_2O reduction, which is completely abolished in cells grown at pH 6.5 (Figure 2). This clearly indicates that the N_2OR produced in these cells is not active. A similar conclusion was obtained from gas measurements performed in other microorganisms, such as *P. denitrificans* [42], *Ensifer meliloti* 1021 [60] and *P. stutzeri* [61], grown at acidic pHs, which evidences a clear impair of the denitrification pathway at acidic pH values, leading to release of N_2O to the environment.

Effect of pH on nitrous oxide reductase

The inability of cells grown at pH 6.5 to reduce N_2O means that N_2OR is not present in an active form *in vivo*, which cannot be attributed to a deficient transcription of *nosZ* (Figure

1A). To explain this result, two hypotheses were investigated: i) effect of pH on the transcription of accessory factors proposed to be involved in the biogenesis of N_2OR copper centers, and ii) the biochemical properties of N_2OR isolated from cells grown at different pH values.

In *M. hydrocarbonoclasticus* the expression levels of *pCuC*, *senC* and *nosL*, which have been proposed to be involved in copper insertion into N_2OR [30, 50], were low but not significantly altered at suboptimal pH to raise the hypothesis that copper centers in *M. hydrocarbonoclasticus* would be affected in terms of copper content. In fact, N_2ORs isolated from *M. hydrocarbonoclasticus* grown at different pH values have spectroscopic features for the presence of CuA and "CuZ" centers fully loaded with copper.

However, although copper content was not affected, the form of "CuZ" center present in N_2OR isolated from cells grown at pH 6.5 ($N_2OR_{6.5}$) differed from the one in $N_2OR_{7.5}$ and $N_2OR_{8.5}$, being mainly CuZ(4Cu1S) in the former and CuZ(4Cu2S) in the later. Thus, lowering the environmental pH influences either maturation of "CuZ" center or its maintenance in an active state.

Towards this end, the gene expression of *nosX* homologue, *MARHY1380*, was analyzed, as it is involved in the maturation of NosR by donating its flavin group to this protein [28]. This gene is highly expressed during the first 3 h in all the growths, but in the growth at pH 6.5 this was also the time point at which *nosR* attained its maximum expression, while in the other two growths the maximum expression occurred at later time-points. This raises the question as whether NosR is fully functional in the cells grown at pH 6.5.

One question that remains to be answered is why the enzyme that presents higher specific activity *in vitro* either using an artificial electron donor or cytochrome c_{552} (its physiological electron donor) was isolated from cells not able to reduce N_2O. The specific activity of N_2OR with "CuZ" center as CuZ(4Cu2S) does not explain the reduction rate of the cells from which

it was isolated. In fact, considering that there is 100 % recovery of N_2OR, isolated from cells grown at pH 7.5, 40 µL of cell suspension would have 0.000104 mg of N_2OR, thus since this volume of cells have a reduction rate of 3.4 x 10^{-2} $\mu mol_{N2O} \cdot min^{-1}$, this gives an estimate of 326 $\mu mol_{N2O} \cdot min^{-1} \cdot mg_{N2OR}^{-1}$. Another important comment is that the K_M for N_2O (18 ± 5 µM) of cells grown at pH 7.5 is similar to the one determined for N_2OR with "CuZ" center as CuZ(4Cu1S) in the fully reduced state using reduced methyl viologen as an electron donor (14 µM) [49]. Therefore, these results clearly point out that N_2OR is activated *in vivo* through a still unknown mechanism, that seems to include the reduction of "CuZ" center to the [$4Cu^{1+}$] oxidation state. In fact, [$4Cu^{1+}$] can be an intermediate in the catalytic cycle as its turnover number is the only one that explains the activity of the whole-cells (320 s^{-1}, determined *in vitro* [22]).

This activation mechanism might consist in a sulfur displacement aid by accessory protein(s), that are membrane associated, as N_2O reduction rate of the periplasm prepared under anaerobic conditions (2.5 ± 0.3 $\mu mol_{N2O} \cdot min^{-1} \cdot mg_{Total}^{-1}$) is lower than the one of a cell extract prepared in the same conditions (3.5 ± 0.4 $\mu mol_{N2O} \cdot min^{-1} \cdot mg_{Total}^{-1}$), and its activity decays with time [62]. A plausible candidate is NosR, an integral membrane protein, shown to be required to isolate N_2OR with "CuZ" center as CuZ(4Cu2S), and to sustain a high activity *in vivo* [63]. N_2OR isolated from cells grown at suboptimal pH ($N_2OR_{6.5}$) is spectroscopically similar to the one isolated from *nosR* mutant strains [27]. Therefore, in *M. hydrocarbonoclasticus* cells grown at pH 6.5, NosR might be inhibited, misfolded or incorrectly maturated (e.g., without the flavin group), or its interaction with N_2OR impaired (as it is known that in *P. aeruginosa* these proteins are part of a supramolecular complex [64]).

Conclusions

The results presented clearly show that N_2OR with "CuZ" center as CuZ(4Cu2S) is a protective form of this enzyme, and that it requires activation to attain maximum activity. Environmental pH, which was mimicked here by growing *M. hydrocarbonoclasticus* at a constant pH, had a clear effect in the ability of the cells to reduce N_2O. Two clear effects were observed in N_2OR: one is the smaller amount of copper-loaded enzyme in the cells grown at pH 6.5 and the other is the form of "CuZ" center present in the isolated enzyme from these cells. The first can be explained by a post-transcriptional regulation, either by its transport to the periplasm by the Tat system or partial assembly of copper centers, as only copper-loaded N_2OR was isolated. The second effect can be attributed to an impair in some accessory factor that is required to maintain N_2OR in an active state or be involved in its activation but is absent or not fully functional in the cells grown at suboptimal conditions.

In conclusion, this study contributes to the identification and understanding of the molecular mechanisms underlying the released of one of the most worrying greenhouse gases of the 21st century, nitrous oxide, due to the acidification of soils and aquatic environments, strengthening the need to develop mitigation processes to decrease its release and its atmospheric concentrations.

Funding

We thank Fundação para a Ciência e Tecnologia for the financial support through the project PTDC/BIA-PRO/098882/2008 (SRP) and PTDC/BBB-BQB/0129/2014 (IM), and the scholarship SFRH/BD/87898/2012 (CC). This work was supported by the Applied Molecular Biosciences Unit – UCIBIO and Associate Laboratory for Green Chemistry - LAQV, which is financed by national funds from FCT (UIDB/04378/2020 and UIDB/50006/2020, respectively).

Conflicts of interest / Competing interests

The authors declare no conflict of interest.

Author Contributions

CC performed the anaerobic purifications; the spectroscopic characterization and all the activity assays. CC and RFN performed the growths in the bioreactor, and nitrate/nitrite quantifications. OM has performed the transcriptional analysis. IM critically read the manuscript. SRP has designed and supervised the experiments and data analysis. CC and SRP wrote the manuscript and analyzed and interpreted the data.

References

1. Le Treut H, Somerville R, Cubasch U, Ding Y, Mauritzen C, Mokssit A, Peterson T and Prather M (2007) In: A. Baede and D. Griggs (eds) Climate Change 2007: The Physical Science Basis Contribution of Working Group I to the Fourth Assessment Report of the Intergovernmental Panel on Climate Change. Cambridge University Press, Cambridge, United Kingdom and New York, NY, USA.,

2. Fowler D, Coyle M, Skiba U, Sutton MA, Cape JN, Reis S, Sheppard LJ, Jenkins A, Grizzetti B, Galloway JN, Vitousek P, Leach A, Bouwman AF, Butterbach-Bahl K, Dentener F, Stevenson D, Amann M and Voss M (2013) The global nitrogen cycle in the twenty-first century. Philos Trans R Soc Lond B Biol Sci 368:20130164

3. Mosier A, Carolien K, Cindy N, Oene O and Sybil S (1998) Closing the global n_2o budget : Nitrous oxide emissions through the agricultural nitrogen cycle inventory methodology. Nutr Cycling Agroecosyst 52:225-248

4. Lassey K and Harvey M (2007) In: M. Harvey (ed). pp. 10-11

5. Thomson AJ, Giannopoulos G, Pretty J, Baggs EM and Richardson DJ (2012) Biological sources and sinks of nitrous oxide and strategies to mitigate emissions. Philos Trans R Soc Lond B Biol Sci 367:1157-1168

6. Voss M, Bange HW, Dippner JW, Middelburg JJ, Montoya JP and Ward B (2013) The marine nitrogen cycle: Recent discoveries, uncertainties and the potential relevance of climate change. Philos Trans R Soc Lond B Biol Sci 368:20130121

7. Richardson D, Felgate H, Watmough N, Thomson A and Baggs E (2009) Mitigating release of the potent greenhouse gas N_2O from the nitrogen cycle - could enzymic regulation hold the key? Trends Biotechnol 27:388-397

8. Zumft WG (1997) Cell biology and molecular basis of denitrification. Microbiol Molec Biol Rev 61:533-616

9. Philippot L (2002) Denitrifying genes in bacterial and archaeal genomes. Biochim Biophys Acta 1577:355-376

10. Zumft WG and Kroneck PM (2007) Respiratory transformation of nitrous oxide (N_2O) to dinitrogen by bacteria and archaea. Adv Microb Physiol 52:107-227

11. Pauleta SR, Carepo MSP and Moura I (2019) Source and reduction of nitrous oxide. Coord Chem Rev 387:436-449

12. Hallin S, Philippot L, Loffler FE, Sanford RA and Jones CM (2018) Genomics and ecology of novel N_2O-reducing microorganisms. Trends Microbiol 26:43-55

13. Scott RA, Zumft WG, Coyle CL and Dooley DM (1989) *Pseudomonas stutzeri* N_2O reductase contains CuA-type sites. Proc Natl Acad Sci U S A 86:4082-4086

14. Brown K, Djinovic-Carugo K, Haltia T, Cabrito I, Saraste M, Moura JJG, Moura I, Tegoni M and Cambillau C (2000) Revisiting the catalytic CuZ cluster of nitrous oxide (N_2O) reductase. Evidence of a bridging inorganic sulfur. J Biol Chem 275:41133-41136

15. Simon J, Einsle O, Kroneck PM and Zumft WG (2004) The unprecedented *nos* gene cluster of *Wolinella succinogenes* encodes a novel respiratory electron transfer pathway to cytochrome *c* nitrous oxide reductase. FEBS Lett 569:7-12

16. Johnston EM, Dell'Acqua S, Ramos S, Pauleta SR, Moura I and Solomon EI (2014) Determination of the active form of the tetranuclear copper sulfur cluster in nitrous oxide reductase. J Am Chem Soc 136:614-617

17. Dell'Acqua S, Pauleta SR, Moura JJ and Moura I (2012) Biochemical characterization of the purple form of *Marinobacter hydrocarbonoclasticus* nitrous oxide reductase. Philos Trans R Soc Lond B Biol Sci 367:1204-1212

18. Rasmussen T, Berks BC, Butt JN and Thomson AJ (2002) Multiple forms of the catalytic centre, CuZ, in the enzyme nitrous oxide reductase from *Paracoccus pantotrophus*. Biochem J 364:807-815

19. Fujita K, Chan JM, Bollinger Ja, Alvarez ML and Dooley DM (2007) Anaerobic purification, characterization and preliminary mechanistic study of recombinant nitrous oxide reductase from *Achromobacter cycloclastes*. J Inorg Biochem 101:1836-1844

20. Pomowski A, Zumft WG, Kroneck PMH and Einsle O (2011) N_2O binding at a 4Cu:2S copper-sulphur cluster in nitrous oxide reductase. Nature 477:234-237

21. Prudêncio M, Pereira AS, Tavares P, Besson S, Cabrito I, Brown K, Samyn B, Devreese B, Van Beeumen J, Rusnak F, Fauque G, Moura JJ, Tegoni M, Cambillau C and Moura I (2000) Purification, characterization, and preliminary crystallographic study of copper-containing nitrous oxide reductase from *Pseudomonas nautica* 617. Biochemistry 39:3899-3907

22. Dell'acqua S, Pauleta SR, Monzani E, Pereira AS, Casella L, Moura JJ and Moura I (2008) Electron transfer complex between nitrous oxide reductase and cytochrome c_{552} from

Pseudomonas nautica: Kinetic, nuclear magnetic resonance, and docking studies. Biochemistry 47:10852-10862

23. Ghosh S, Gorelsky SI, Chen P, Cabrito I, Moura JJG, Moura I and Solomon EI (2003) Activation of N_2O reduction by the fully reduced micro4-sulfide bridged tetranuclear CuZ cluster in nitrous oxide reductase. J Am Chem Soc 125:15708-15709

24. Chan JM, Bollinger J, Grewell CL and Dooley DM (2004) Reductively activated nitrous oxide reductase reacts directly with substrate. J Am Chem Soc 126:3030-3031

25. Carreira C, Dos Santos MMC, Pauleta SR and Moura I (2020) Proton-coupled electron transfer mechanisms of the copper centres of nitrous oxide reductase from *Marinobacter hydrocarbonoclasticus* - An electrochemical study. Bioelectrochemistry 133:107483

26. Wunsch P and Zumft WG (2005) Functional domains of nosr, a novel transmembrane iron-sulfur flavoprotein necessary for nitrous oxide respiration. J Bacteriol 187:1992-2001

27. Wunsch P, Körner H, Neese F, van Spanning RJ, Kroneck PM and Zumft WG (2005) NosX function connects to nitrous oxide (N_2O) reduction by affecting the Cu(Z) center of NosZ and its activity *in vivo*. FEBS Lett 579:4605-4609

28. Zhang L, Trncik C, Andrade SLA and Einsle O (2017) The flavinyl transferase ApbE of *Pseudomonas stutzeri* matures the NosR protein required for nitrous oxide reduction. Biochim Biophys Acta 1858:95-102

29. Wallenstein MD, Myrold DD, Firestone M and Voytek M (2006) Environmental controls on denitrifying communities and denitrification rates: Insights from molecular methods. Ecol Appl 16:2143-2152

30. Sullivan MJ, Gates AJ, Appia-Ayme C, Rowley G and Richardson DJ (2013) Copper control of bacterial nitrous oxide emission and its impact on vitamin B_{12}-dependent metabolism. Proc Natl Acad Sci U S A 110:19926-19931

31. Smid AE and Beauchamp EG (1976) Effects of temperature and organic matter on denitrification in soil. Can J Soil Sci 56:385-391

32. Saggar S, Jha N, Deslippe J, Bolan NS, Luo J, Giltrap DL, Kim DG, Zaman M and Tillman RW (2013) Denitrification and N_2O:N_2 production in temperate grasslands: Processes, measurements, modelling and mitigating negative impacts. Sci Total Environ 465:173-195

33. Bergaust L, van Spanning RJM, Frostegard A and Bakken LR (2012) Expression of nitrous oxide reductase in *Paracoccus denitrificans* is regulated by oxygen and nitric oxide through FnrP and NNR. Microbiology 158:826-834

34. Hassan J, Qu Z, Bergaust LL and Bakken LR (2016) Transient accumulation of NO_2^- and N_2O during denitrification explained by assuming cell diversification by stochastic transcription of denitrification genes. PLoS Comput Biol 12:e1004621

35.. Blum JM, Su Q, Ma Y, Valverde-Perez B, Domingo-Felez C, Jensen MM and Smets BF (2018) The pH dependency of N-converting enzymatic processes, pathways and microbes: Effect on net N_2O production. Environ Microbiol 20:1623-1640

36. Liu B, Frostegard A and Bakken LR (2014) Impaired reduction of N_2O to N_2 in acid soils is due to a posttranscriptional interference with the expression of *nosZ*. MBio 5:e01383-01314

37. Liu B, Mørkved PT, Frostegård A and Bakken LR (2010) Denitrification gene pools, transcription and kinetics of NO, N_2O and N_2 production as affected by soil pH. FEMS Microbiol Ecol 72:407-417

38. Imek M and Cooper JE (2002) The influence of soil pH on denitrification: progress towards the understanding of this interaction over the last 50 years. Eur J Soil Sci 53:345-354

39. Wan R, Wang L, Chen Y, Zheng X, Su Y and Tao X (2018) Insight into a direct carbon dioxide effect on denitrification and denitrifying bacterial communities in estuarine sediment. Sci Total Environ 643:1074-1083

40. Spiro S (2012) Nitrous oxide production and consumption: Regulation of gene expression by gas-sensitive transcription factors. Philos Trans R Soc Lond B Biol Sci 367:1213-1225

41. Torres MJ, Simon J, Rowley G, Bedmar EJ, Richardson DJ, Gates AJ and Delgado MJ (2016) Nitrous oxide metabolism in nitrate-reducing bacteria: Physiology and regulatory mechanisms. Adv Microb Physiol 68:353-432

42. Bergaust L, Mao Y, Bakken LR and Frostegård A (2010) Denitrification response patterns during the transition to anoxic respiration and posttranscriptional effects of suboptimal pH on nitrous oxide reductase in *Paracoccus denitrificans*. Appl Environ Microbiol 76:6387-6396

43. Alves T, Besson S, Duarte LC, Pettigrew GW, Girio FM, Devreese B, Vandenberghe I, Van Beeumen J, Fauque G and Moura I (1999) A cytochrome *c* peroxidase from *Pseudomonas nautica* 617 active at high ionic strength: Expression, purification and characterization. Biochim Biophys Acta 1434:248-259

44. Untergasser A, Cutcutache I, Koressaar T, Ye J, Faircloth BC, Remm M and Rozen SG (2012) Primer3—new capabilities and interfaces. Nucleic Acids Res 40:e115-e115

45. Gomes JP, Hsia RC, Mead S, Borrego MJ and Dean D (2005) Immunoreactivity and differential developmental expression of known and putative *Chlamydia trachomatis* membrane proteins for biologically variant serovars representing distinct disease groups. Microbes Infect 7:410-420

46. Lowry OH, Rosebrough NJ, Farr AL and Randall RJ (1951) Protein measurement with the Folin phenol reagent. J Biol Chem 193:265-275

47. Hanna PM, Tamilarasan R and McMillin DR (1988) Cu(I) analysis of blue copper proteins. Biochem J 256:1001-1004

48. Kristjansson JK and Hollocher TC (1980) First practical assay for soluble nitrous oxide reductase of denitrifying bacteria and a partial kinetic characterization. J Biol Chem 255:704-707

49. Carreira C, Mestre O, Nunes RF, Moura I and Pauleta SR (2018) Genomic organization, gene expression and activity profile of *Marinobacter hydrocarbonoclasticus* denitrification enzymes. PeerJ 6:e5603

50. Bennett SP, Soriano-Laguna MJ, Bradley JM, Svistunenko DA, Richardson DJ, Gates AJ and Le Brun NE (2019) NosL is a dedicated copper chaperone for assembly of the CuZ center of nitrous oxide reductase. Chem Sci 10:4985-4993

51. Bertsova YV, Fadeeva MS, Kostyrko VA, Serebryakova MV, Baykov AA and Bogachev AV (2013) Alternative pyrimidine biosynthesis protein ApbE is a flavin transferase catalyzing covalent attachment of FMN to a threonine residue in bacterial flavoproteins. J Biol Chem 288:14276-14286

52. Pauleta SR and Moura I (2017) In: R. A. Scott (ed) Encyclopedia of inorganic and bioinorganic chemistry. pp. 1-11

53. Carreira C, Pauleta SR and Moura I (2017) The catalytic cycle of nitrous oxide reductase - the enzyme that catalyzes the last step of denitrification. J Inorg Biochem 177:423-434

54. Ghosh S, Gorelsky SI, George, DeBeer S, Chan JM, Cabrito I, Dooley DM, Moura JJG, Moura I and Solomon EI (2007) Spectroscopic, computational, and kinetic studies of the mu4-sulfide-bridged tetranuclear CuZ cluster in N_2O reductase: pH effect on the edge ligand and its contribution to reactivity. J Am Chem Soc 129:3955-3965

55. Hahnke SM, Moosmann P, Erb TJ and Strous M (2014) An improved medium for the anaerobic growth of *Paracoccus denitrificans* Pd1222. Front Microbiol 5:18

56. Baumann B, van der Meer JR, Snozzi M and Zehnder AJ (1997) Inhibition of denitrification activity but not of mRNA induction in *Paracoccus denitrificans* by nitrite at a suboptimal pH. Anton Leeuw Int J G 72:183-189

57. Hartop KR, Sullivan MJ, Giannopoulos G, Gates AJ, Bond PL, Yuan Z, Clarke TA, Rowley G and Richardson DJ (2017) The metabolic impact of extracellular nitrite on aerobic metabolism of *Paracoccus denitrificans*. Water Res 113:207-214

58. Almeida JS, Julio SM, Reis MA and Carrondo MJ (1995) Nitrite inhibition of denitrification by *Pseudomonas fluorescens*. Biotechnol Bioeng 46:194-201

59. Schreiber F, Wunderlin P, Udert KM and Wells GF (2012) Nitric oxide and nitrous oxide turnover in natural and engineered microbial communities: Biological pathways, chemical reactions, and novel technologies. Front Microbiol 3:372

60. Bueno E, Mania D, Frostegard A, Bedmar EJ, Bakken LR and Delgado MJ (2015) Anoxic growth of *Ensifer meliloti* 1021 by N_2O-reduction, a potential mitigation strategy. Front Microbiol 6:537

61. Firth JR and Edwards C (1999) Effects of cultural conditions on denitrification by *Pseudomonas stutzeri* measured by membrane inlet mass spectrometry. J Appl Microbiol 87:353-358

62. Carreira C (2017) Dept Química. Universidade Nova de Lisboa, Caparica, pp. 264

63. Wunsch P, Herb M, Wieland H, Schiek UM and Zumft WG (2003) Requirements for Cu(A) and Cu-S center assembly of nitrous oxide reductase deduced from complete periplasmic enzyme maturation in the nondenitrifier *Pseudomonas putida*. J Bacteriol 185:887-896

64. Borrero-de Acuna JM, Rohde M, Wissing J, Jansch L, Schobert M, Molinari G, Timmis KN, Jahn M and Jahn D (2016) Protein network of the *Pseudomonas aeruginosa* denitrification apparatus. J Bacteriol 198:1401-1413

Tables

Table 1 - Purification yield and copper ratio of *M. hydrocarbonoclasticus* N_2OR isolated from the growths carried out at pH 6.5, 7.5 and 8.5.

Sample	Yield ($mg_{N2OR} \cdot L^{-1}$)	Yield[a] ($mg_{N2OR} \cdot g_{cell}^{-1}$)	Cu/protein[b]
$N_2OR_{6.5}$	0.5 ± 0.2	0.16 ± 0.02	3.6 ± 0.1
$N_2OR_{7.5}$	2.6 ± 0.4	0.5 ± 0.2	5.5 ± 0.4
$N_2OR_{8.5}$	1.1 ± 0.2	0.3 ± 0.1 [c]	3.1 ± 0.2

Notes: [a] Yield is given as mg of purified N_2OR per g of wet cell; [b] Considering N_2OR as a monomer.

Table 2 - Activities of *M. hydrocarbonoclasticus* N_2OR, isolated from the growth performed at pH 6.5, 7.5 and 8.5, using cytochrome c_{552} and methyl viologen as electron donors.

Sample	Methyl viologen (incubation 3 h) ($\mu mol_{N2O} \cdot min^{-1} \cdot mg_{N2OR}^{-1}$)	Cytochrome c_{552} ($\mu mol_{N2O} \cdot min^{-1} \cdot mg_{N2OR}^{-1}$)
$N_2OR_{6.5}$	192 ± 14	1.25 ± 0.07[a]
$N_2OR_{7.5}$	51 ± 18	0.004 ± 0.001[b]
$N_2OR_{8.5}$	55 ± 5	-

Notes: [a] Reduction rates of N_2OR in the fully reduced state; [b] Reduction rates of N_2OR reduced with sodium dithionite, as explained in Materials and Methods.

Figure legends

Fig. 1 Representative gene expression profile of *narG* (closed diamonds), *nirS* (open squares), *c-norB* (closed triangles) and *nosZ* (open circles) encoding the catalytic domain of *M. hydrocarbonoclasticus* denitrification enzymes during growth at pH 6.5 (Panel A) and 8.5 (Panel B), under denitrifying conditions. Relative expression values were obtained by normalizing expression of each gene, analyzed by *q*PCR, to the reference gene *16S rRNA* gene. The growth curve obtained for each growth conditions is represented in grey as $\log OD_{600\ nm}$.

Fig. 2 Representative profile of *M. hydrocarbonoclasticus* denitrification metabolites and enzymatic activities at (A) pH 6.5 and (B) pH 8.5. Nitrate (closed diamonds) and nitrite (open squares) concentrations at different time-points of the growth are represented in the primary axis and nitric oxide (closed triangles) and nitrous oxide (open circles) reduction rates by whole-cells are represented in the secondary axis. The growth curve obtained for each growth conditions is represented in grey as $\log OD_{600\ nm}$.

Fig. 3 Visible and X-band EPR spectra of *M. hydrocarbonoclasticus* N_2OR isolated from growths performed at different pH values: (A, B) $N_2OR_{6.5}$, (C, D) $N_2OR_{7.5}$ and (E, F) $N_2OR_{8.5,}$ in 100 mM Tris-HCl pH 7.6. For each nitrous oxide reductase sample, the spectra of the fully oxidized form with potassium ferricyanide (solid line - I), as-isolated (dotted-dashed line - II), dithionite-reduced form (dashed line - III) and methyl viologen (IV) are presented. The contribution of methyl viologen radical to the spectrum was removed (*). The visible spectrum of $N_2OR_{8.5}$ (E, III) starts at 540 nm to remove the contribution of contaminant

cytochrome that is more evident in the reduced form. The extinction coefficient was determined based on the copper content of the samples.

Figures

Figure 1

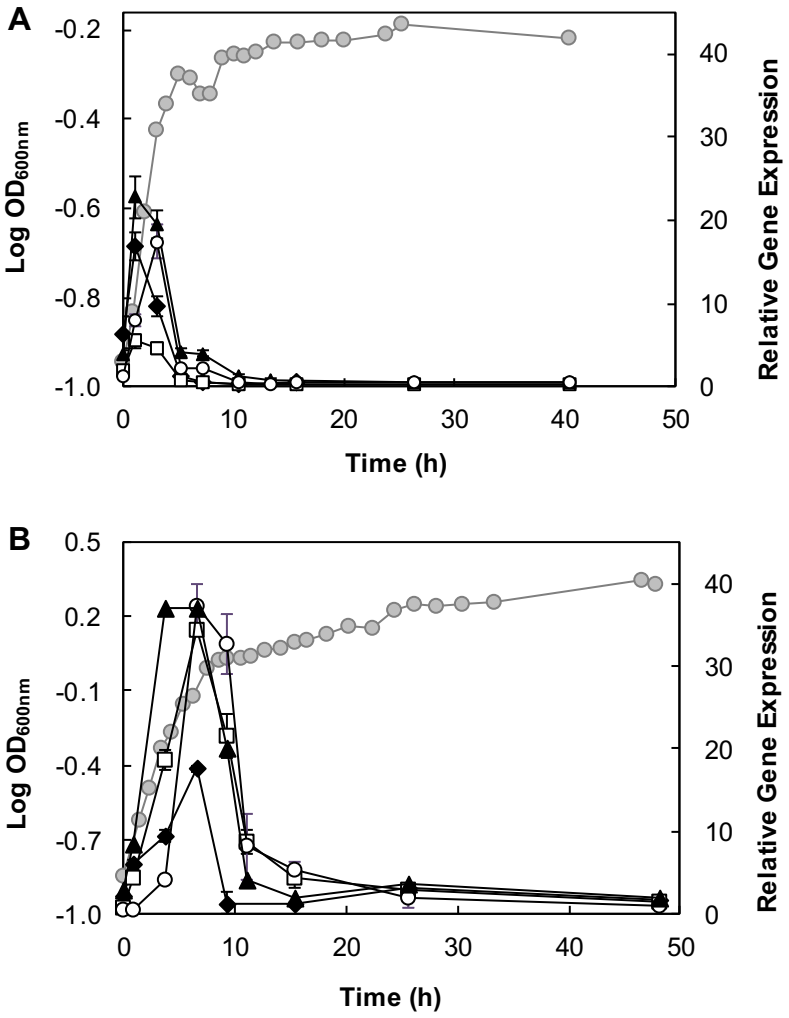

Figure 2

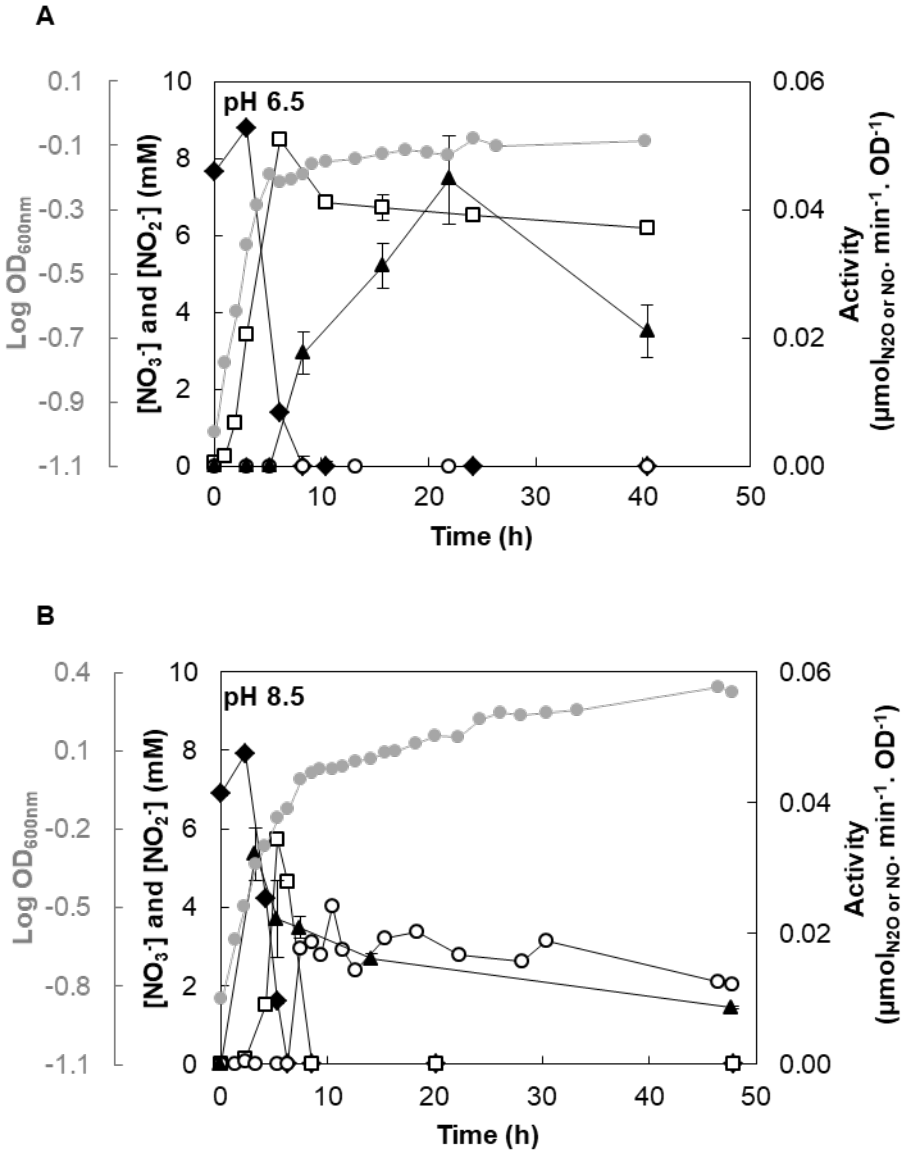
A
pH 6.5
Log OD600nm
[NO3-] and [NO2-] (mM)
Activity (µmolN2O or NO. min-1. OD-1)
Time (h)
B
pH 8.5
Log OD600nm
[NO3-] and [NO2-] (mM)
Activity (µmolN2O or NO. min-1. OD-1)
Time (h)

Figure 3

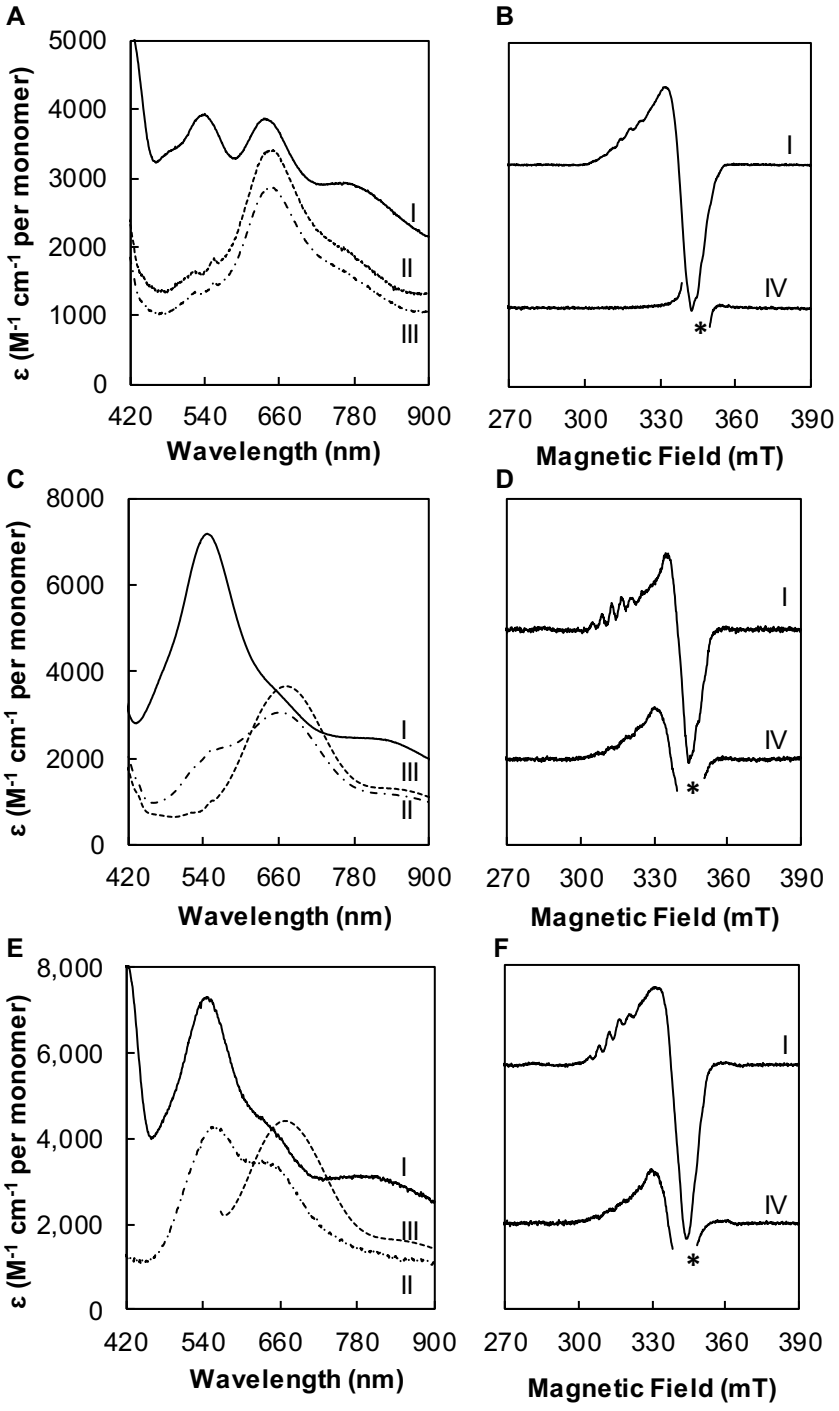
A
B
C
D
E
F
ε (M-1 cm-1 per monomer)
Wavelength (nm)
Magnetic Field (mT)
I
II
III
IV
*
5000
4000
3000
2000
1000
0
8000
6000
8,000
6,000
4,000
2,000
420
540
660
780
900
270
300
330
360
390